Rock and Soil Mechanics

Volume 43 | Issue 4 Article 7

6-9-2022

Prediction of water inflow in water-sealed oil storage caverns based on fracture seepage effect

Zhong-ming JIANG
Key Laboratory of Water-Sediment Sciences and Water Disaster Prevention of Hunan Province, Changsha University of Science & Technology, Changsha, Hunan 410114, China

Zhe-zhen XIAO
School of Hydraulic Engineering, Changsha University of Science & Technology, Changsha, Hunan 410114, China

Dong TANG
Key Laboratory of Dongting Lake Aquatic Eco-Environmental Control and Restoration of Hunan Province, Changsha University of Science & Technology, Changsha, Hunan 410114, China

Guo-fu HE
SINOPEC Shanghai Engineering Ltd. Company, Shanghai 200120, China

See next page for additional authors

Custom Citation

JIANG Zhong-ming, XIAO Zhe-zhen, TANG Dong, HE Guo-fu, XU Wei, . Prediction of water inflow in water-sealed oil storage caverns based on fracture seepage effect[J]. Rock and Soil Mechanics, 2022, 43(4): 1041-1047.

Prediction of water inflow in water-sealed oil storage caverns based on fracture seepage effect

Authors

Zhong-ming JIANG, Zhe-zhen XIAO, Dong TANG, Guo-fu HE, and Wei XU

Rock and Soil Mechanics 2022 43(4): 1041−1047 ISSN 1000−7598
https: //doi.org/10.16285/j.rsm.2021.6217 rocksoilmech.researchcommons.org/journal

Prediction of water inflow in water-sealed oil storage caverns based on fracture seepage effect

JIANG Zhong-ming[1, 2], XIAO Zhe-zhen[1], TANG Dong[1, 3], HE Guo-fu[4], XU Wei[5]

1. School of Hydraulic Engineering, Changsha University of Science & Technology, Changsha, Hunan 410114, China
2. Key Laboratory of Water-Sediment Sciences and Water Disaster Prevention of Hunan Province, Changsha University of Science & Technology, Changsha, Hunan 410114, China
3. Key Laboratory of Dongting Lake Aquatic Eco-Environmental Control and Restoration of Hunan Province, Changsha University of Science & Technology, Changsha, Hunan 410114, China
4. SINOPEC Shanghai Engineering Ltd. Company, Shanghai 200120, China
5. PowerChina Zhongnan Engineering Corporation Limited, Changsha, Hunan 410014, China

Abstract: The accurate prediction on the spatial distribution of water inflow and seepage characteristics in the cavern is one of the basic tasks to ensure the safety and economy during construction and operation of the underground water-sealed oil cavern. In order to study the seepage effect of randomly distributed fractures in the surrounding rock of underground water-sealed oil storage cavern on water inflow prediction and spatial distribution of seepage field, a seepage analysis method of fractured rock mass based on embedded fracture element (EFE) is proposed to analyze the three-dimensional seepage field in Zhanjiang water-sealed oil storage caverns. The reliability of the proposed method is validated by the measured data and calculated results, and then the water inflow of the this project during the operation period is predicted. The calculation results show that the EFE model can well simulate the influence of fractures on the local seepage field of fractured rock mass, and reflect the non-uniformity of spatial distribution of the seepage field and water inflow in caverns. The research results can provide references for the precise design of seepage control measurements for water-sealed caverns and the design of sewage treatment facilities during the operation period.

Keywords: underground oil storage caverns; fractured rock mass; embedded fracture element model; anisotropy; water inflow

1 Introduction

Under the influence of various geological processes, the complex fracture networks occur in the underground rock mass, causing a very complicated seepage situation in the underground oil storage in cavern area. In order to ensure the water sealing effect of the underground oil storage in rock caverns and accurately predict the water inflow during the construction and operation periods, it is necessary to analyze the complex spatial and temporal variation of the seepage field in the underground water-sealed oil cavern. The latest edition of "Standard for design of underground oil storage in rock caverns" (GB50455-2020) [1] proposed that the water seepage volume of the treated caverns should not exceed 200 m^3/d for the storage capacity of 1 million m^3. The surrounding rock with excessive leakage should be treated with specific seepage control measures to reduce the water inflow of the cavern, thereby reducing the requirements for the surface sewage treatment capacity. Meanwhile, the groundwater level above the storage area should maintain a certain height to ensure the water sealing performance of the cave.

The prediction of water inflow in underground caverns mainly includes hydrogeological comparison method, empirical formula method[2], analytical formula method[3−4] and numerical calculation method[5−12]. The hydrogeological comparison method predicts the total water inflow of the planned underground engineering by comparing the similar projects with similar geological conditions, which has a certain reference value. The empirical formula method and the analytical formula method propose the relevant formulas for solving the water inflow in the cavern to provide theoretical basis and preliminary design indicators of the engineering. However, the above methods are difficult to accurately predict the uneven spatial distribution characteristics of the water inflow in the cavern[8], and it is difficult to evaluate the influence of the water curtain system on the water inflow. A scientific and reasonable numerical method of fracture seepage will overcome the shortcomings of the above methods. If more details are considered in the simulation, the numerical simulation method will be better than the analytical method for predicting the spatial distribution of water inflow in the cavern. For example, Liu et al.[5] used a discrete fracture network

Received: 04 August 2021 Revised: 17 September 2021
This work was supported by the National Natural Science Foundation of China (52178381, 51778070).
First author: JIANG Zhong-ming, male, born in 1969, PhD, Professor, PhD supervisor, mainly engaged in teaching and scientific research in geotechnical engineering. E-mail: zzmmjiang@163.com

seepage model to simulate the water inflow in the underground powerhouse. Lu et al.[6] studied the influence of a single seepage fissure on the water inflow of the cavern. Jia et al.[7] adopted the random field theory to reflect the difference of permeability coefficient in the formation and predicted the water inflow of the cavern.

The Zhanjiang underground water-sealed oil storage cavern is taken as an example to study the seepage characteristics by combining the embedded fractured element (EFE) model[13] and the equivalent continuum model. The three-dimensional seepage field of the water-sealed oil cavern is analyzed in detail to calculate the size and spatial distribution of the water inflow in the cavern. For the EFE seepage analysis model, the discrete fractures are used to divide specific fracture units, and the equivalent hydraulic parameters of the fracture units are calculated according to the geometric characteristics of the discrete fractures. The EFE units are regarded as anisotropic seepage model units to reflect the anisotropic properties of seepage in fractured rock mass.

2 Analysis method of water inflow in cavern

For practical engineering, the rock mass generally contains different scales of fractures or fissures. Under the current technical conditions, it is difficult to incorporate all the fissures into the seepage model. Therefore, under the premise of ensuring the calculation efficiency and accuracy, the long and large seepage fissures obtained by engineering surveying and mapping are considered, while the small and micro-fissure networks that are not detected by surveying and mapping, are embedded in the effective continuum media by the REV (representative element volume). In order to analyze the seepage effect of fractured rock mass, Jiang et al.[13] developed an EFE model analysis method in FLAC^{3D} simulator. The core idea of this method is described below. For the rock mass with cracks, the permeability is often affected by many factors including the occurrence, density of the cracks. Therefore, the anisotropic model can be used to describe the permeability or the anisotropic seepage properties of the rock mass. Based on the discrete fracture network (DFN) function provided in the FLAC^{3D}5.0 version and the built-in FISH language, the FISH function for calculating the anisotropic permeability of fracture elements is compiled, and the independent discrete fracture network is integrated with the entity of FLAC^{3D} to realize the fracture seepage analysis. The seepage anisotropy of the EFE model is described by the seepage tensor formula and the derivation process can be seen in Jiang et al[13].

$$K_{ij} = K_{\mathrm{r}} + n_{\mathrm{f}}\left(K_{\mathrm{f}ij} - K_{\mathrm{r}}\right) \quad (1)$$

where K_{ij} is the permeability coefficient of the saturated rock mass; K_{r} is the permeability coefficient of the saturated rock block; $K_{\mathrm{f}ij}$ is the contribution of fractures to the unit permeability tensor; n_{f} is the area fracture ratio in the seepage direction. The subscript i and j represent the direction, and takes 1, 2, and 3; the subscript r represents the rock block or the intact rock, and the subscript f represents the structural surface such as the fissure.

At first, the discrete cracks shown in Figure 1(a) are generated near the surrounding rock of the cavern through the crack data obtained by the underground survey. Then, the EFE is generated based on the discrete cracks in the above model, as shown in Figure 1(b), in which the red element is the embedded fractured element. After the seepage calculation, the total water inflow of the cavern is obtained by extracting the unbalanced flow at the node of the cave wall in Figure 1(c). In the above analysis process, the fracture width can be adjusted to control the permeability difference of the fractured element, that is, different fractures adopt different permeability coefficients.

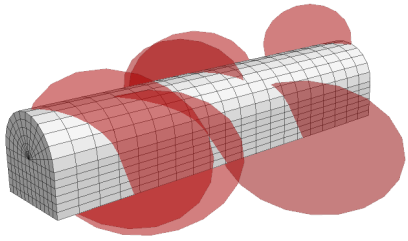

(a) Discrete fractures

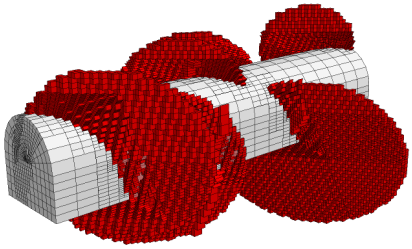

(b) EFE model

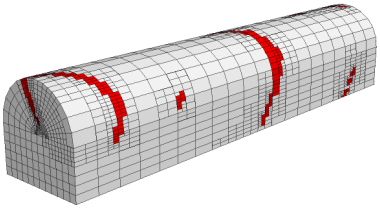

(c) EFE distribution in the cavern wall

Fig. 1 Schematic of EFE model generation

3 Case study

3.1 Project overview

The designed storage capacity of Zhanjiang underground oil storage cavern is 500×10^4 m^3. The

underground engineering mainly includes 3 construction tunnels, 10 main caverns, 16 shafts and 8 water curtain tunnels. The main caverns are arranged in the form of parallel along the direction of NE10°. The design length and span are 923 m and 20 m, respectively. The cave height and the bottom elevation are 30 m and −110.0 m, respectively. The cross-sectional shape is a straight wall circular arch. The designed clear spacing between the main cavern wall and the adjacent construction roadway wall is 30 m, and the designed net spacing between two adjacent main caverns is 40 m. The floor elevation of the water curtain tunnel is −55.0 m, all of which are straight walls and circular arches. The water injection holes are set in water curtain tunnels 1 to 6 with a hole spacing of 10 m and an elevation of −53.5 m. The hole length covers 10 m outside the cavern wall.

3.2 Hydrogeological condition

The water levels of wells and the surface water bodies in the oil storage area and the surrounding region were surveyed and measured before and during the construction of the engineering. The buried depth of the groundwater table is generally 0.04−11.9 m, and the elevation is 4.6−24.18 m. The change of groundwater table is basically consistent with the topography. According to the geological survey, geophysical prospecting and drilling data, there are 3 faults (F1, F2 and F3) in the oil storage area and the affected areas. F1 is a regional large fault, located 150−200 m in the northern part of the oil storage area; F2 is a secondary minor fault, which obliquely penetrates the entire oil storage cavern area from northwest to southeast; and F3 is a regional small fault, which obliquely passes the southeast of the oil storage cavern from southwest to northeast. According to the statistical results of construction geology, the fractured water in the rock mass ooze, or drip, even discharge in line form from the surface of the vault of the main caverns. The seepage sections are all related to the joint plane, and seepage mainly occurs along the joint plane or joint group. The main seepage sections and the distribution of structural planes are shown in Fig. 2.

3.3 Analysis of water inflow from the cavern

He[14] used the hydrogeological analogy method, empirical analysis method and other methods to estimate the water inflow of the Zhanjiang underground water sealed oil storage cavern. He compared the underground water sealed LPG (liquefied oil gas) cavern in Guangzhou Shantou with the Zhanjiang oil storage cavern and concluded that the water inflow during the construction period of the cavern would reach 14,000 m^3/d, and the stable water inflow was 1,250 m^3/d. The total water inflow of the cavern at the initial stage of construction was 1 425.1 m^3/d, and the total water inflow of the cavern during the operation period was 395.9 m^3/d estimated by using the empirical formula of Hiroshi Oshima[15]. The total water inflow volume of the cavern in the initial stage of construction and during the operation period were 1418.7 m^3/d and 553.8 m^3/d, respectively, by using the analytical formula of Sato Kuniaki [15]. The total stable water inflow of the cavern was 798.33 m^3/d by using the numerical method, and the total water inflow of the cavern when the water curtain was replenished during the operation period was 595.29 m^3/d.

Since the roof of the main cavern of this project had not been excavated when the literature [14] was written, the seepage fissures exposed by the main cavern was not fully considered, the permeability coefficient of the surrounding rock was thereby lower than that of the actual situation, resulting in a smaller estimate value of the water inflow.

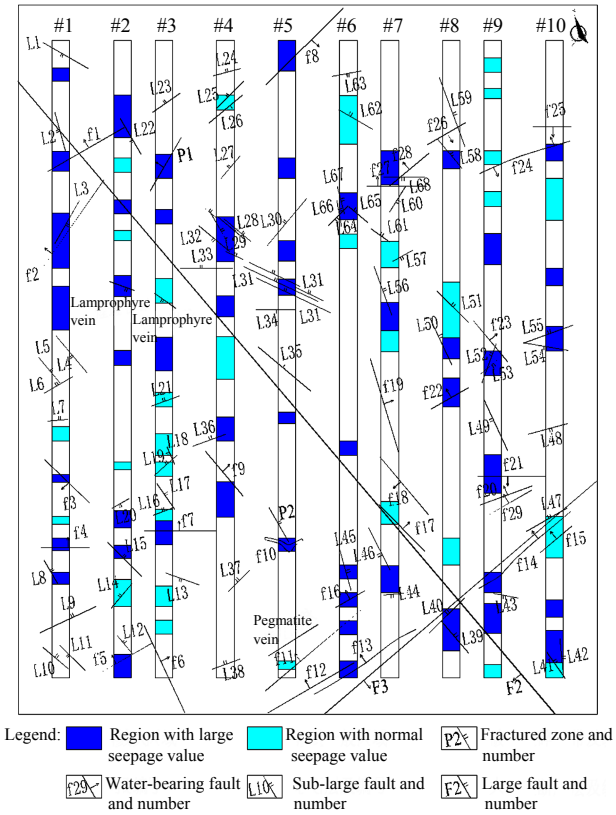

Fig. 2 Distribution of main seepage sections and structural planes on the roof of the main cavern

3.3.1 Numerical model and parameters setup

According to the engineering geological report, the corresponding numerical model is established as shown in Fig. 3. The southwest corner of the #1 main cavern is set as the origin in the numerical model and the right-hand coordinate system is applied. The positive *Y* direction is the northeast direction along the axis of

the cavern. The model includes 10 main caverns and 8 water curtain tunnels, of which the maximum elevation of the roof of the cavern is 80.0 m, and the bottom elevation of the cavern is −110.0 m. The effects of two large faults traversing the storage area are taken into account in the numerical model. The numerical model is 1 900 m×2 000 m, and the boundary of the model is about 500 m from the outer edge of the cavern. The elevation of the lowest part of the model is −270 m. The numerical model has a total of 416,812 nodes and 1,374,147 elements.

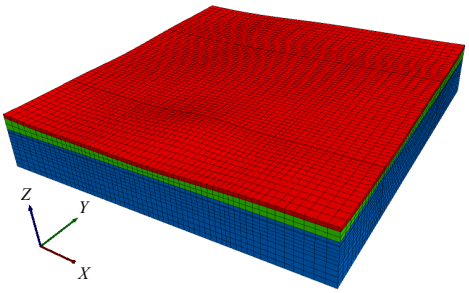

(a) Computational grids

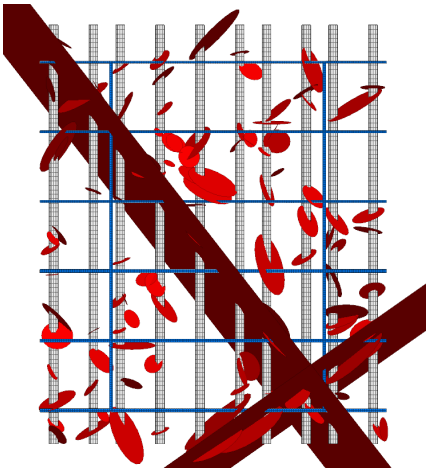

(b) Distribution of faults and fractures

Fig. 3 Numerical model

The vertical boundary of the model is assumed to be the fixed water head boundary. The bottom horizontal boundary is set as an impermeable boundary. The cavern wall adopts the free seepage boundary. The water curtain roadway filled with water is set as the fixed water head boundary. According to the groundwater level monitoring data and the hydrogeological survey data at the periphery of the reservoir area, the initial groundwater level shown in Figure 4 was fitted.

The water pumping-out test was carried out when the borehole was drilled to 3 m of the slightly weathered layer during the exploration process. The permeability coefficient obtained from the test was in the range of 10^{-2} and 10^{-3} m/d, implying that the rock was in moderately weathered or much more highly weathered state. According to the results of the water injection-fallback test of the water curtain holes during the construction period, the average permeability coefficient of the water curtain holes is about 1.728×10^{-2} m/d. Judging from the results of the water injection test in the borehole, the permeability coefficient of the slightly weathered rock mass is mostly in the range of 10^{-3} and 10^{-2} m/d, and the permeability coefficient of the surrounding rock is 9×10^{-4} m/d. If the slightly weathered rock mass is regarded as an equivalent isotropic rock mass, the permeability coefficient is about 1.35×10^{-3} m/d considering that the water-conducting structure above the −120 m elevation in the oil cavern is relatively developed.

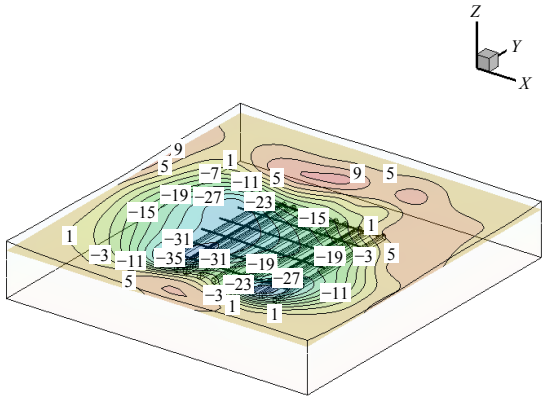

Fig. 4 Initial groundwater surface

The permeability of surrounding rock at different burial depths in the model is considered by partition and layer. In Scheme 1, the equivalent continuum model is adopted in the area not passed through by the fractures, which is regarded as the isotropic material, and the values of the parameters in each layer are shown in Table 1, where the hybrid model is calculated using both the EFE model and the equivalent continuum model. The area penetrated by the fissures adopts the EFE model and it is regarded as the anisotropic material. The permeability coefficient of the fissures in the cavern is inversely analyzed according to the measured water inflow. The permeability coefficients of structural surfaces with different grades in each area after grouting is calculated based on the cubic law.

Table 1 Permeability coefficient

Strata	Model	Permeability coefficient /(m • d^{-1})
Moderately weathered rock mass and overburden	Isotropic model	1.73×10^{-2}
	Hybrid model	1.73×10^{-2}
Slightly weathered rock mass above −120 m	Isotropic model	1.35×10^{-3}
	Hybrid model	9×10^{-4}
Slightly weathered rock mass below −120 m	Isotropic model	9×10^{-4}
	Hybrid model	9×10^{-4}

Four numerical simulation schemes and parameters

are provided in Table 2. Scheme 1 and Scheme 2 are compared to illustrate the superiority of the EFE model. They also used to select the rational permeability coefficients in the prediction and analysis of water inflow during operation (Scheme 3 and Scheme 4).

Table 2 Computational schemes

Schemes	Seepage model	Study stage	Water replenishment pressure /MPa
1	Hybrid model	Construction period	0.30
2	Isotropic model	Construction period	0.30
3	Hybrid model	Operation period	0.01
4	Hybrid model	Operation period	0.30

In order to test the effectiveness of the EFE model in the seepage field, the steady-state seepage simulations were carried out in two different conditions of Scheme 1 and Scheme 2 based on the observation data of the oil cavern area in June 2019. The initial groundwater table is shown in Fig. 4. Some water curtain holes were sealed, and the water supply pressure in the water curtain tunnel and the remaining water curtain holes is 0.3 MPa.

The Schemes 3 and 4 were used to examine the influence of the replenishment pressure on the water inflow and the seepage field of the cavern area during operation period. The replenishment pressures of the water curtain holes were 0.01 MPa and 0.3 MPa, respectively. The maximum water level in the construction tunnel is −49 m. The part of gallery inside of the seal plug and main caverns were filled with oil. The top surface elevation of the crude oil was −81 m, and the operation pressure of 0.018 MPa was applied on the oil surface at the same time. The permeability coefficients in schemes 3 and 4 were the same as that of scheme 1.

3.3.2 Model validation and comparison

The project contains 10 main caverns. The representative #5 main cavern and the transverse section in the middle of the oil cavern area were selected to analyze the water pressure under Scheme 1 and 2, as shown in Figs. 5 and 6. The white areas in Figs. 5 and 6 are the unsaturated zone, also called the drained zone. It shows that Scheme 1 has obvious uneven distribution of seepage field because the seepage effect of fractures is considered.

The water pressure profile at 1 m above the roof of the #5 main cavern is plotted in Fig.7. The starting point and the ending point of the survey line are located at the south end and north end of the roof of the #5 main cavern. The resistance of the water pressure in the water curtain hole in the transmission path along the crack is far less than that in the complete rock mass[16], resulting in significant differences in the distribution of water pressure in the rock mass above the roof of cavern, as shown in the calculation results of scheme 1 in Fig. 7. Since the influence of fracture seepage effect is considered in calculation scheme 1, while not considered in calculation scheme 2, thus, the water pressure above the cavern calculated according to scheme 2 is far less than that calculated according to scheme 1, and its variation range is very small, even under the condition of the same replenishment pressure of water curtain hole and the same total water inflow of the cavern. This shows that the better the uniformity of rock mass, the more uniform the distribution of water pressure above the oil storage cavern.

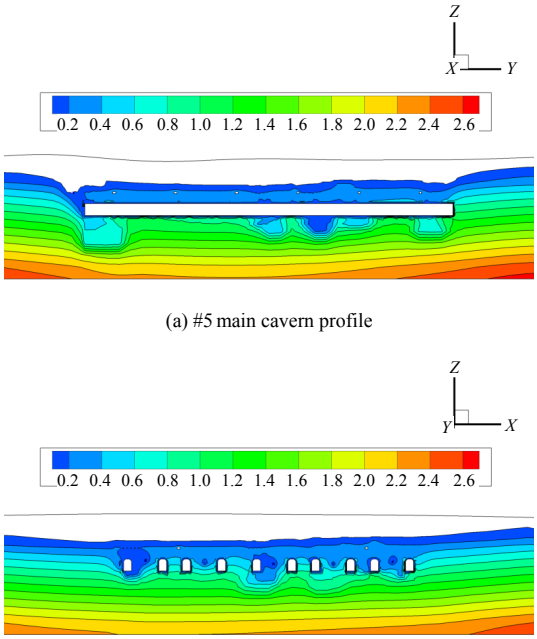

(a) #5 main cavern profile

(b) Transverse section in the middle of oil cavern area

Fig. 5 Water pressure distribution in Scheme 1 (unit: MPa)

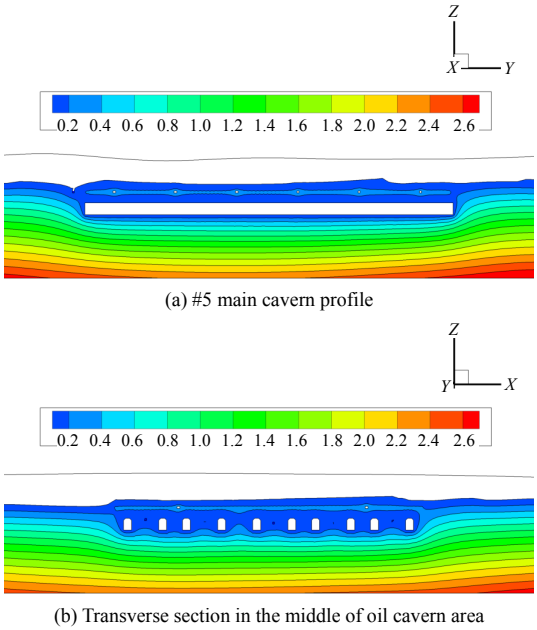

(a) #5 main cavern profile

(b) Transverse section in the middle of oil cavern area

Fig. 6 Water pressure distribution in scheme 2 (unit: MPa)

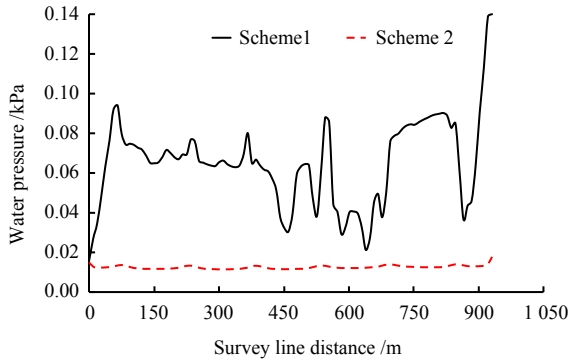

Fig. 7 Water pressure distribution at the roof of #5 cavern

Figure 7 also shows that the water pressure at the roof of the cave in the EFE model is much larger than that by the homogeneous model. The reason is attributed to the fact that the fractures have stronger permeability and the water flow resistance is small, which results in a better pressure transfer. Since the EFE model more realistically reflects the seepage field distribution in the surrounding rock of the cavern, the error between the calculated result and the real value is relatively smaller than that of the equivalent continuum model. It is therefore more reasonable to use the EFE model to estimate the water sealing performance of the water-sealed oil storage cavern.

Table 3 shows the statistics of the water inflow in the caverns calculated for Scheme 1 and Scheme 2 and the measured water inflow in the cavern. Figure 8 is the bar chart comparing the estimated water inflow and the measured water inflow between the Scheme 1 and the Scheme 2. The calculated results show that the total water inflow of the cavern obtained by the Scheme 1 and Scheme 2 are 2478.5 m^3/d and 2491.6 m^3/d respectively, and the errors between these two schemes and the measurements are 0.10% and 0.43%, respectively, which are both highly consistent with the measured value. This shows that it can obtain the total water inflow almost the same as the measured value by adjusting the permeability coefficient in the calculated model. Although the total water inflow obtained by the above two analysis methods is basically the same, the water inflow between the caverns obtained in the Scheme 1 is obviously different. It has the similar distribution law as the measured value. The error between the calculated value of water inflow in each cavern and the measured value is mostly between 1% and 4%. The water inflow of #1 main cavern is as high as 542.5 m^3/d, followed by the water inflow of the main caverns #2, #4, #5, #6 and #10, while the water inflow of the main caverns of #3, #7, #8 and #9 is relatively small (less than 200 m^3/d). The difference between the water inflow of each cavern obtained by the Scheme 2 is relatively small, but the error between the measured water inflow of each cavern and estimated value mostly varies between 20% and 70%, and the error is obviously larger than that of Scheme 1, which verifies the rationality of the EFE model.

Table 3 Water inflow analysis from different caverns

Cavern No.	Water inflow /(m^3 • d^{-1})			Error /%	
	Measured value	Calculated value			
		Scheme 1	Scheme 2	Scheme 1	Scheme 2
#1	550	542.5	280.3	−1.36	−49.04
#2	396	400	221.8	1.01	−43.99
#3	175	174.5	226	−0.29	29.14
#4	205	211.3	256.3	3.07	25.02
#5	200	200.6	259.9	0.30	29.95
#6	195	199.4	231.6	2.26	18.77
#7	163	156.8	232.9	−3.80	42.88
#8	135	133.8	235.5	−0.89	74.44
#9	148	151.2	237.5	2.16	60.47
#10	314	308.3	309.7	−1.82	−1.37
Total water inflow	2481	2478.5	2491.6	−0.10	0.43

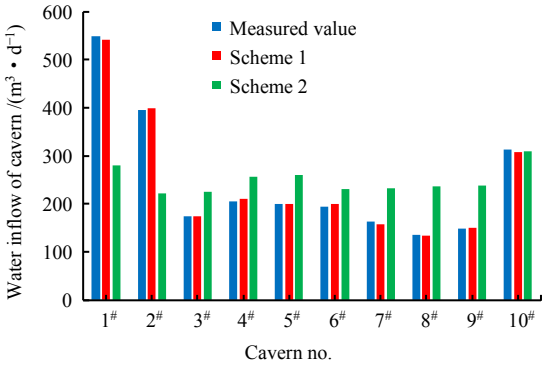

Fig. 8 Water inflow analysis from different caverns

It can be inferred that the EFE model can well simulate the flow difference between caverns in the seepage analysis of water-sealed oil caverns, if relatively rich geological data can be obtained.

3.3.3 Calculation of water inflow during operation period

The prediction of water inflow during the operation period is estimated using the fracture permeability coefficient determined in Scheme 1. Figure 9 is the water pressure profile in the middle of the cavern area under Scheme 3 and Scheme 4. The water pressure above the cavern in Scheme 3 with 0.01 MPa replenishment pressure is significantly lower than that in Scheme 4 with 0.3 MPa replenishment pressure, so the water sealing performance of the cavern is better under the condition of high pressure replenishment. Table 4 shows the predicted water inflow during the operation period. When the flow rate of the cavern tends to be stable, the total water inflow of the cavern in Scheme 3 is 619.1 m^3/d, while the total inflow of the cavern in Scheme 4 reaches 1509.5 m^3/d. It can be seen that the

water inflow from the cavern is much greater under the condition of high-pressure water replenishment than that of the low-pressure replenishment condition. According to the current specifications, for oil storage caverns with a total storage capacity of 500×10^4 m^3, the total water inflow should not exceed 1000 m^3/d. If the high-pressure water replenishment scheme is adopted, the sewage treatment capacity of the oil storage cavern needs to be increased.

Figure 10 is the water pressure profile of the #5 main cavern at 1 m above the cavern roof of Scheme 3 and Scheme 4. The starting point of the survey line is at the southern roof the #5 main cavern, and the end point of the survey line is at the northern roof of the #5 main cavern. It can be found that there are similar distribution trends of water pressure above the cavern roof in the Scheme 3 with the 0.01 MPa replenishment pressure and the Scheme 4 with the 0.3 MPa replenishment pressure. Overall, the water pressure of Scheme 3 is lower, but the water pressure at some fissures is the same as that of Scheme 4, indicating that the water pressure transfer effect of the fracture is very significant.

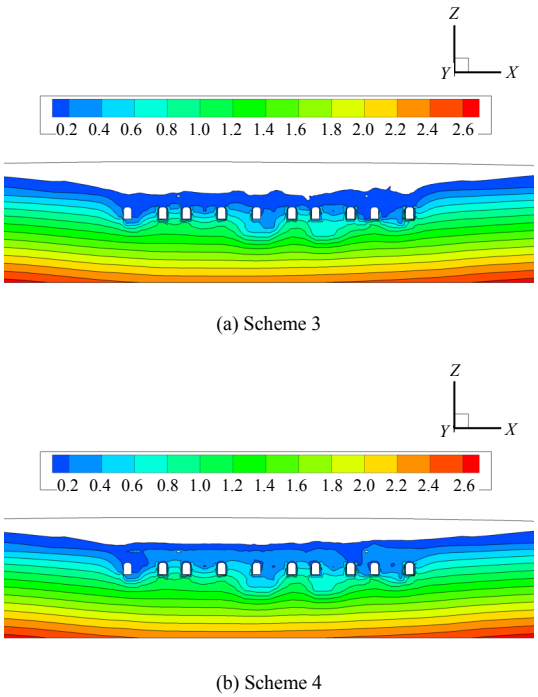

(a) Scheme 3

(b) Scheme 4

Fig. 9 Water pressure distribution of mid-section of caverns during operation (unit: MPa)

Table 4 Cavern water inflow during operation (unit: m^3/d)

Schemes	Total water inflow	#1	#2	#3	#4	#5	#6	#7	#8	#9	#10
3	619.1	132.2	35.5	51.7	51.5	56.1	42.8	52.7	27.4	56.9	112.2
4	1 509.5	339.2	155.4	114.2	146.2	109.3	112.1	98.6	80.4	110.6	243.5

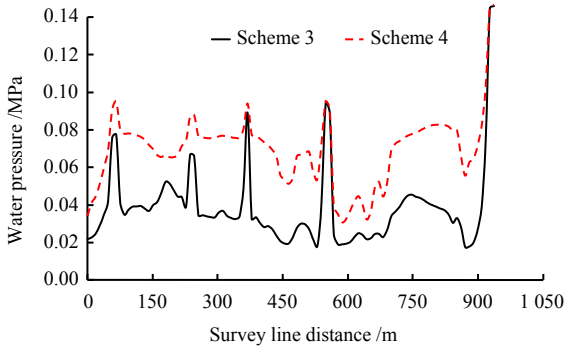

Fig. 10 Water pressure distribution at the roof of #5 cavern during operation

4 Conclusions

During the construction of large underground water-sealed oil caverns, the change of seepage field will directly affect the water sealing effect of the cavern. The analysis of seepage flow can provide a basis for the subsequent water seepage treatment work and the selection of sewage treatment system equipment capacity. In this paper, the EFE model is used to simulate the seepage of fissures, and the seepage characteristics in the water-sealed oil cavern are studied to obtain some main conclusions as follows:

(1) Considering the fissures and structural surfaces exposed in the cavern, combined with the hydrogeological data, the EFE model and the equivalent continuum model are used to calculate the seepage field in the oil cavern. The results show that the EFE model can reflect the real situation of the seepage field in the oil cavern area, and its water inflow prediction results are closer to the actual situation.

(2) The EFE model can simulate the replenishment water flows into the cavern from the water curtain holes and the water curtain roadway along the fissures. The uneven distribution of the seepage field in the oil cavern area caused by the fissures can also be simulated. After analyzing the main seepage structural surfaces, the EFE model can well simulate the flow difference of each cavern, and its calculation results are also consistent with the actual situation.

(3) The water flowing fissures can better reflect the water replenishment effect of the water curtain. The EFE model is used to predict the water inflow of each cavern during the operation period of the water-sealed oil cavern, which can provide the technical support for the accurate design of the cavern seepage treatment.

References

[1] Sinopec Group. GB/T 50455−2020 Standard for design

of underground oil storage in rock caverns[S]. Beijing: China Planning Press, 2020.

[2] ZHANG Ji-xun, YANG Fan, YANG Ling, et al. Improved water seepage prediction in petroleum cavern group[J]. Journal of China Three Gorges University (Natural Sciences), 2017, 39(2): 14−18.

[3] CUI Jing-hao. Underground engineering and urban disaster prevention[M]. Beijing: China Water & Power Press, 2007.

[4] FU He-lin, AN Peng-tao, LI Kai, et al. Analysis of influence of surrounding rock heterogeneity on water inrush in tunnel[J]. Rock and Soil Mechanics, 2021, 42(6): 1519−1528.

[5] LIU Ze-jun, HUANG Yong. Forecasting water yeild of underground powerhouse based on fractured network seepage model[J]. Water Resources and Power, 2010, 28(8): 58−60, 170.

[6] LU Wen-long, ZHOU Zhi-fang, HUANG Yong. Effect of single fractured zone on water inflow of undergroud unlined cavern[J]. Yellow River, 2014, 36(2): 112−114.

[7] JIA Chao, WANG Lun-xiang, WANG Zhe-chao, et al. Prediction of water inflows in underground caverns based on the random field theory[J]. Modern Tunnelling Technology, 2015, 52(5): 117−124.

[8] WANG Zhe-chao, LI Shu-cai, LIANG Jian-yi, et al. Prediction and measurement of groundwater flow rate of underground crude oil storage caverns[J]. Chinese Journal of Geotechnical Engineering, 2014, 36(8): 1490−1497.

[9] CUI Shao-dong, GUO Shu-tai, GAO Jian-feng. Research on water inflow into underground water sealed cave based on unsaturated flow[J]. Chinese Journal of Underground Space and Engineering, 2017, 13(Suppl. 2): 746−751.

[10] PANG Jia-wei, DING Guo-ping, CHEN Gang, et al. Numerical analysis of drawdown and water inflow of underground water-sealing oil storage in rock caverns[J]. Oil & Gas Storage and Transportation, 2013, 32(9): 1007−1011, 1017.

[11] YAN Dong-qing, REN Xu-hua, ZHANG Ji-xun, et al. Analysis of impact of artificial water curtains on water inflow of water sealed undergroud petroleum storage caverns[J]. Journal of China Three Gorges University (Natural Sciences), 2014, 36(1): 15−18.

[12] WANG Z C, KWON SANGKI, QIAO L P, et al. Estimation of groundwater inflow into an underground oil storage facility in granite[J]. Geomechanics and Engineering, 2017, 12(6). DOI: 10.12989/gae.2017. 12.6. 1003.

[13] JIANG Zhong-ming, XIAO Zhe-zhen, TANG Dong. Numerical analysis method of fluid flow in fractured rock mass of dam foundation[J]. Journal of Hydraulic Engineering, 2020, 51(10): 1289−1298.

[14] HE Guo-fu. Prediction and analysis of water inflow in an underground water-sealed cavern in Zhanjiang[J]. West-China Exploration Engineering, 2011, 23(11): 19−24, 33.

[15] El TANI M. Circular tunnel in a semi-infinite aquifer[J]. Tunneling and Underground Space Technology, 2003, 18(1): 49−55.

[16] LI Shu-cai, WANG Zhe-chao, PING Yang, et al. Discrete element analysis of hydro-mechanical behavior of a pilot underground crude oil storage facility in granite in China[J]. Tunnelling and Underground Space Technology, 2014, 40: 75−84.